



Research article

Harnessing salinity gradient energy: Pushing forward in water reclamation via on-site reverse electro dialysis technology

Tamara Sampedro^a, Elisa Mazo^b, Lucía Gómez-Coma^a, Axel Arruti^c, Marcos Fallanza^a, Javier Pinedo^c, Javier Rioyo^b, María Sainz^b, Raquel Ibañez^a, Inmaculada Ortiz^{a,*}

^a Universidad de Cantabria, Department of Chemical and Biomolecular Engineering, Av. Los Castros 46, 39005, Santander, Spain

^b MARE, Ctra. Torres - Reocín, Bo La Barquera 13, 39311, Cartes, Spain

^c APRIA Systems S.L. Pol. Ind. de Morero, Parcela, 2-13, Nave 3-8, 39611, Guarnizo, Spain

ARTICLE INFO

Keywords:

Water reclamation
Reverse electro dialysis
Salinity gradient energy
Electro-membrane process

ABSTRACT

Effluents from urban wastewater treatment plants (UWWTPs) discharged into water bodies such as the sea or ocean, offer a potential source of renewable energy through the salinity gradient (SGE) between seawater and treated water. The European project Life-3E: Environment-Energy-Economy aims to demonstrate an innovative process integrating renewable energy production with water reclamation. Using reverse electro dialysis (RED) technology, SGE can power tertiary wastewater treatment processes in coastal UWWTPs, offsetting energy costs associated with water regeneration and reuse.

This study pioneers a pilot-scale RED system with a 20.125 m² membrane area at a coastal UWWTP in Comillas, Spain. The initial tests with synthetic solutions in the up-scaled RED module have reached a peak power density of 1.39 W/m². Under real environmental conditions, using natural seawater and treated water at ambient temperatures (289 ± 0.5 K), the system achieved a peak power density of 0.95 W/m², outperforming previous setups in stability and efficiency.

The results show competitive energy metrics, with an energy efficiency of 1.9 W/m²·m³LC and up to 38.2 Wh/m³LC generated. The treated water, with an inlet conductivity to the RED stack of <1 mS/cm, exits the pilot with a conductivity of around 4 mS/cm (measured under a load of 2A and a flow rate of 500 L/h), maintaining the quality standards for urban reuse.

This study demonstrates the effective integration of RED technology into water reclamation stages, creating a self-sustained energy loop and enhancing the efficiency in water management. By harnessing blue energy and supporting sustainable water reuse, this research contributes to the global shift toward a circular water economy and critical sustainability goals.

1. Introduction

The inefficient consumption and management of freshwater resources is placing substantial strain on natural renewable reservoirs, leading to a widening gap between water supply and demand (Kakwani and Kalbar, 2024). The strategies aimed at ensuring a water secure future supply of this essential need to the population, turn around the planned recycling of wastewater fractions of domestic/urban, industrial, agricultural, and stormwater basis (United Nations Environment Programme, 2023). Nevertheless, only 58% of generated wastewater was properly treated in 2022, revealing a lack of significant progress towards the Sustainable Development Goal 6 (SDG 6) (United Nations, 2023).

In this context, the advance in water remediation is an increasingly pressing global need, driven by the growing rates of urbanization and industrialization (United Nations, 2024). Therefore, water reclamation plants play a crucial role in mitigating the environmental impact of effluents generated by diverse human activities (Jones et al., 2022).

In 2020, global total freshwater withdrawals amounted to 3881 billion cubic meters (FAO of the United Nations, 2024). Furthermore, the water demand is projected to continue increasing at a rate of approximately 1% annually (United Nations, 2021). Hence, addressing future demands will rely significantly on reintroducing regenerated wastewater into the water cycle boundaries (WWAP, 2017). Currently, the volume of wastewater generated worldwide from domestic and

* Corresponding author.

E-mail address: ortizi@unican.es (I. Ortiz).

<https://doi.org/10.1016/j.jenvman.2024.123251>

Received 28 June 2024; Received in revised form 20 September 2024; Accepted 3 November 2024

Available online 11 November 2024

0301-4797/© 2024 The Authors. Published by Elsevier Ltd. This is an open access article under the CC BY-NC-ND license (<http://creativecommons.org/licenses/by-nc-nd/4.0/>).

urban uses is estimated at 360 billion cubic meters per year (Jones et al., 2021), of which approximately only 11% is treated and intentionally reused (United Nations Environment Programme, 2023). Therefore, there is still considerable scope to move further towards water reclamation boost for different uses.

However, increasing the expansion of planned water recycling is predominantly constrained upon the implementation of regeneration treatments aimed at enhancing the physicochemical quality of effluents from Wastewater Treatment Plants (WWTPs). Concurrently, the interdependence of the water-energy nexus hinders the adoption of more exhaustive purification processes enabling reclamation, owing to an additional energy consumption (Cardoso et al., 2021; Tow et al., 2021). The electricity demands of wastewater treatment plants represent approximately 25% of the total energy consumed within the water sector (International Energy Agency, 2018). Nonetheless, in addressing the water-energy nexus, the pursuit of renewable energy sources aims to reconcile both issues and provide integrated and complementary solutions (Li et al., 2024; UN environment programme, 2023).

Salinity gradient energy, often termed "blue energy," is a sustainable energy source that leverages the difference in salt concentration between two bodies of water, such as seawater and freshwater. The concept of utilizing this energy stems from the natural mixing process that occurs when these two types of water come into contact (Pattle, 1954). It has been reported that up to 18 GW of SGE could be harnessed derived from the salinity gap between seawater and treated wastewaters at their discharge points (Logan and Elimelech, 2012). Moreover, the theoretical potential of harvestable blue energy ranges from 0.4 kWh/m³ to 0.8 kWh/m³ (Chae et al., 2023; Choi et al., 2024).

Reverse electrodialysis (RED) has emerged as a prominent method to harness this energy by exploiting the ionic movement caused by concentration differences (Mejía-Marchena et al., 2023). In a RED system, alternating cation and anion exchange membranes are placed between streams of high-salinity (seawater) and low-salinity (freshwater) solutions. The difference in concentration creates a driving force that causes ions to migrate from the more concentrated solution to the less concentrated one. As these ions pass through their respective selective membranes, a potential difference is created, which can be converted into electrical energy. This method represents a promising alternative for capturing the significant energy potential available at locations where freshwater and seawater naturally mix, such as river mouths, estuaries or WWTPs discharge points (Rastgar et al., 2023).

The performance of RED systems is determined by several factors, including the characteristics of the ion-exchange membranes, such as their selectivity and resistance, as well as the system configuration. The flow rates of the solutions, membrane arrangement, and the optimization of the stack design are also critical to maximizing energy efficiency. Although RED holds great promise, technical challenges remain, particularly in reducing energy losses due to membrane resistance and preventing fouling (Hong and Park, 2023), which can impact system performance and cost-effectiveness.

Building upon prior studies conducted by the research group, as successfully demonstrated by Gómez-Coma et al. (2020) at laboratory scale with natural seawater and wastewater solutions, reverse electrodialysis membrane-technology showcases its potential for power generation, reaching up to 1.43 W/m². Furthermore, the harvested SGE can be used to facilitate tertiary treatment processes which are often constrained by their additional energy requirements, thereby enabling advanced purification processes for water reclamation.

Advancing further, the viability of RED for energy extraction at pilot plant scale has also been demonstrated. Tedesco et al. (2017) documented the operation of a RED prototype with an effective membrane cell pair area of approximately 220 m². The study employed synthetic brine (3.5M NaCl) and brackish water (0.01M NaCl) streams, revealing that under optimal operating conditions, the system achieved a power output of 3.3 W/m². However, experimentation with real water sources yielded no more than 1.4 W/m². In a more recent study, Mehdizadeh

et al. (2021) demonstrated the performance of a RED stack with 90 m² cell pair membrane area. The study reported power outputs of 0.97 W/m² and 0.62 W/m² when exploiting the salinity gradient of synthetic and natural solutions of seawater (0.57M NaCl) and river water (0.004M NaCl) streams, respectively. Considering the performance of a pilot plant-scale RED module in a coastal marine environment similar to the conditions of this study, namely, using real seawater (0.62 M NaCl) and wastewater (0.014M NaCl), the yield reaches a maximum of 0.76 W/m² (Nam et al., 2019).

This underscores the potential for a paradigmatic shift towards a circular economy pattern of the management of water by leveraging its untapped chemical energy through RED. However, the large-scale implementation of RED for SGE harnessing still faces technical and economic challenges (Chae et al., 2023). Specifically, the technical issues are focused on the development of effective cleaning protocols and fouling control strategies (Moreno et al., 2017; Vital et al., 2024). Consequently, to overcome its primary bottlenecks, research in this field is focused on optimizing energy capture under real environments (Tristán et al., 2023), enhancing membrane efficiency, and mitigating associated capital and operational costs (Gurreri et al., 2020; Tufa et al., 2018).

The challenges associated with the efficiency of RED systems, particularly in real-world applications, highlight the necessity of conducting pilot-scale studies. As observed in experiments with RED prototypes, using real water—such as treated wastewater—can result in significant power reductions, sometimes down to 50%, due to issues like membrane fouling and pressure drop (Tedesco et al., 2016). This underscores the importance of moving beyond theoretical models to pilot-scale projects that operate in real environments and use real wastewater streams.

In this context, the LIFE-3E project at the Comillas WWTP in Cantabria, Spain, plays an essential role. The project is designed to reclaim 1 m³/h of treated wastewater for reuse in municipal street and road cleaning (Fig. 1). Additionally, the treated effluent will serve as the low-salinity stream in a RED module. By integrating the RED technology into a real operational environment, the project not only contributes to boost water reclamation but also provides valuable insights into the energy efficiency and challenges of RED in practical applications. This approach is vital for addressing the obstacles identified in previous studies, such as energy loss due to fouling, and for advancing the development of scalable, energy-efficient water reclamation technologies.

The primary goal of this work is to report the design, implementation, and first results of a pilot plant aimed at the recovery of SGE within a wastewater treatment facility. Specific aims comprise assessing the energy efficiency of the reverse electrodialysis process in harnessing the salinity gradient energy emerged at effluent discharge sites. This research will contribute to guide forthcoming studies and technological advancements in the field of blue energy extraction in wastewater treatment plants, highlighting its capacity to assist wastewater reclamation.

2. Methodology

The experimental procedure of this study was specifically designed to ensure the proper functioning of the system and to characterize the performance of the constructed pilot prototype through the study of the influence of operation variables. The research was conducted using both synthetic solutions and real water streams to evaluate the efficiency and scalability of the technology in a real-life environment.

2.1. Site description

The RED pilot plant has been installed at the Comillas' WWTP (Cantabria 43.3895° N, 4.2987° W, Spain). This facility has a treatment capacity of approximately 35,700 population equivalent (p.e.) and is situated near the shoreline of the municipality of Comillas and is bathed

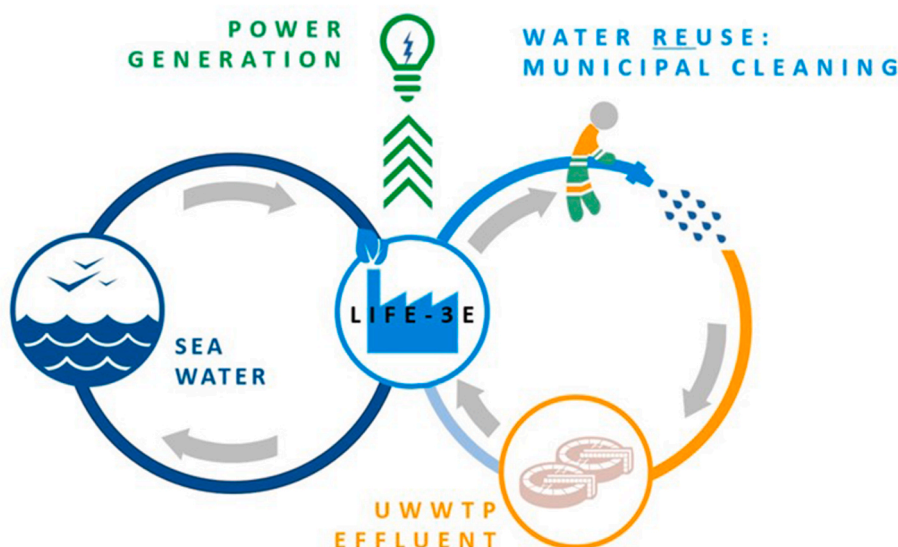


Fig. 1. Scheme of the LIFE 3E – Environment Energy and Economy project concept. (Source: LIFE 3E, 2024).

by the Cantabrian Sea. The WWTP of Comillas has a design capacity for wastewater treatment of 50 m³/h (1200 m³/day). The industrial purification facility includes the following stages in the water treatment line: pre-treatment, sand removal, settling, biological treatment, and tertiary treatment. This final stage consists of a disinfection step with ultraviolet lamps installed in the water line channel and microfiltration at 10 µm using disc filters that operate by gravity. Comillas UWWTP tertiary treatment energy requirement is on average 0.22 kWh per cubic meter of treated wastewater.

2.2. Pilot plant layout and main features

The main layout of the pilot plant and its key components are given in Fig. 2. According to the hydraulic engineering of the prototype, it comprises four hydraulic lines: (1) concentrated stream (HC, seawater); (2) diluted stream (LC, treated wastewater); (3) electrolyte solution; and

(4) cleaning circuit. The HC line includes a pre-treatment process to ensure the quality of the water entering the modules, which consists of two cartridge filters of 50 and 5 µm. In the LC line, in addition to the cartridge filters, installed to prevent biofouling that would compromise the performance of the RED there is also an in-line ultraviolet disinfection stage. Additional pre-treatment has been included in the pilot design as an initial protective measure. However, this pre-treatment will not be necessary during demonstrative activities, as the quality of the treated WW from the UWWTP already meets the required quality standards for RED and water reuse.

2.2.1. RED unit

The pilot-scale setup comprises two reverse electro dialysis units (FuMATech® FT- ED-1750-2-115) manufactured by FuMA-Tech (Functional Membranes and Plant Technology) BWT GmbH® (Germany), with a total effective membrane cell pair area of 20.125 m² for the RED

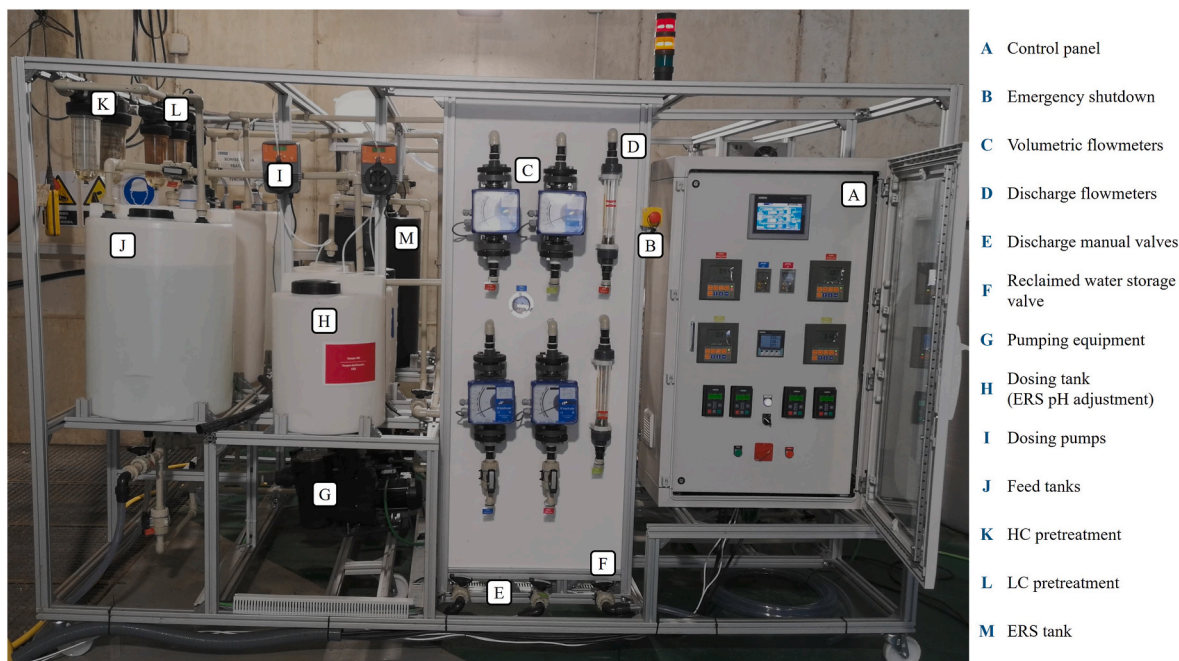


Fig. 2. Front view of the plant and list of the main depicted elements.

Table 1

Characteristics of each commercial RED module manufactured on-demand by Fumatech GmbH® (Germany). CEM Fumasep® FKS-PET-75 and AEM Fumasep® FAS-PET-75.

Component	Parameter	Description	Value	Unit
RED Stack	N_{cp}	Number of cell pairs	115	–
Fumatech GmbH®, Germany	b	Channel width	0.463	m
	L	Channel length	0.378	m
	δ_{sp}	Inter-membrane distance equal to spacer's thickness	270	μm
	ϵ	Spacer porosity	82.5	%
CEM/AEM	R_0	Electrical resistance	<3	$\Omega\cdot\text{cm}^2$
CEM/AEM	δ	Thickness dry	65–90	μm
CEM	α_{CEM}	Permselectivity	>96	%
AEM	α_{AEM}	Permselectivity	>93	%

module. The technical specifications for the FT- ED-1750-2-115 module and the ion exchange membranes (cation exchange membrane fumasep® FKS-PET-75 (CEM); anion exchange membrane fumasep® FAS-PET-75 (AEM) that are inside the 115 cell pairs are listed in Table 1. The electrodes of the RED modules are made of titanium with a DSA® coating.

2.2.2. Pre-treatment procedure

Both feed streams, treated wastewater (WW), LC, and seawater, HC, pass through a safety filtration unit provided with cartridge filters installed in line, Cintropur® model NW25 (Airwatec, S.A.) of 10 μm and 5 μm . In addition, disinfection with an ultraviolet lamp model UV 2100 of Cintropur® (Airwatec, S.A.) with a consumption of 25W and an irradiation wavelength of 253.7 nm is applied to the LC flow in its pathway to the RED module.

2.2.3. Pumping equipment

The HC and LC hydraulic lines are equipped with two pumps from AstralPool, model *Victoria Plus Silent 1/2 CV III* with a nominal flow rate of 10 m^3/h (provided by Fluidra España, S.A.U.).

Regarding the electrode rinse solution and cleaning lines, they are equipped with two pumps model *CM 1–3* from Grundfos and a fixed nominal flow rate of 1.7 m^3/h (Grundfos Holding, A.G.).

2.2.4. Measurement systems and sensors

Voltage measurement and data recording is performed by means of an electronic load from Chroma (Chroma Systems Solutions, Inc.) consisting of a 63103A module and a 6312A central unit. This equipment has a maximum operation power of 300W and allows working in a voltage range of 0–80V and amperage range of 0–60A. The main instrumentation elements for control of the system are: volumetric flow meters SC250 (Tecfluid, S.A.), conductivity meters model *HI7639* (HANNA Instruments®), pH sensors *HI1001* (HANNA Instruments®), pressure transducers *Cerabar PMP11* (Endress + Hauser Group Services AG).

2.2.5. Cleaning procedure

The manufacturer of the membrane module recommends the use of citric acid or potassium hydroxide (up to 10%) as cleaning agents. However, according to the user's manual recommendations, a gentle cleaning with warm demineralized water heated up to 30 °C (module maximum temperature is set at 40 °C) has always been prioritized. The membrane packs were preserved and conditioned by filling the compartments with sodium chloride solution (1.5 wt%).

2.3. Feed solutions

This section details the preparation and characteristics of the solutions used in the experiments, ensuring a comprehensive understanding of the conditions under which the RED system was tested.

2.3.1. Synthetic NaCl solutions

The initial commissioning of the system was conducted using pure sodium chloride synthetic solutions. Commercial NaCl with 99.9% purity from Unión Salinera de España, S.A. was utilized for this purpose. The salinity gradient used for these experiments was kept constant at 0.55 M NaCl for the concentrated compartment and 0.02 M NaCl for the diluted compartment (Ortiz-Martínez et al., 2020).

2.3.2. Engineered synthetic solutions with divalent ions

Subsequently, synthetic solutions were prepared replicating the composition of the main ions in seawater and in the treated WW intended to feed the pilot prototype during the demonstration activities, as presented in Table 2. These solutions were made by dissolving the appropriate salts in demineralized water and storing them in 5 m^3 tanks. The salts used included commercial NaCl (99.9% purity from Unión Salinera de España, S.A.), Na_2SO_4 (99.9% purity from Minera de Santa Marta, S.A.), $\text{CaCl}_2\cdot 2\text{H}_2\text{O}$ supplied by Tetra CC Tech®, and $\text{MgCl}_2\cdot 6\text{H}_2\text{O}$ supplied by Dead Sea Works, LTD.

2.3.3. Real waters

The real seawater has been supplied by the “Oceanographic Center of Santander” (Cantabria, Spain), belonging to the “Spanish Institute of Oceanography”. Seawater is filtered with 25- and 10- μm filtration units and is transported to the Comillas WWTP where it is stored in four tanks of 5 m^3 capacity each that have been installed as part of the project; seawater is pumped from the tanks to the pilot.

The wastewater arriving at the treatment plant has been subjected to the following processes: pretreatment, primary settling, biological treatment (8 biofilters with an average residence time of 8 h) and tertiary treatment. The outlet water from the biofilters is subjected to a disinfection treatment using a set of ultraviolet lamps and stored in a treated water tank from where it is pumped to the effluent discharge point. A part of the treated wastewater receives additional filtration (10 μm) using disc filters for its subsequent use in the cleaning process of the biofilters and other treatment facility cleaning purposes. Prior to pumping the treated WW from the storage tank to the pilot plant, coagulation-flocculation was conducted using aluminium sulphate (at a dosage of 265 mg/L, Acideka, Spain) and cationic polyacrylamide (at a dosage of 2 mg/L, A.E. Vallés, Spain) to effectively remove suspended particles and dissolved organic matter. Subsequently, the treated water underwent a 24-h sedimentation process.

The ion composition in seawater and treated WW is shown in Table 2.

2.3.4. Electrolyte rinse solution

During performance tests, the electrode rinsing electrolyte indicated by the manufacturer in the user manual of the commercial modules has been used; this is a redox pair of potassium ferrocyanide ($\text{K}_4[\text{Fe}(\text{CN})_6] \cdot 3\text{H}_2\text{O}$, 98,5% purity from Thermo Fisher GmbH) and potassium ferricyanide ($\text{K}_3[\text{Fe}(\text{CN})_6]$, 98% purity from Thermo Fisher GmbH), both at a concentration of 0.05M with addition of sodium chloride (NaCl 99,9% purity from Unión Salinera de España, S.A.) at 0.25M.

Table 2
Molar concentration of different ions.

Feed solution	Na^+	Cl^-	Ca^{2+}	Mg^{2+}	SO_4^{2-}
Seawater	0.567 ± 0.293	0.552 ± 0.031	$(1.74 \pm 0.7) \cdot 10^{-2}$	$(6.26 \pm 3) \cdot 10^{-2}$	$(2.56 \pm 0.1) \cdot 10^{-2}$
Reclaimed water	$(2.4 \pm 0.99) \cdot 10^{-3}$	$(2.5 \pm 0.49) \cdot 10^{-3}$	$(3.3 \pm 0.56) \cdot 10^{-4}$	$(3.4 \pm 0.94) \cdot 10^{-4}$	$(3.8 \pm 1) \cdot 10^{-4}$

3. Results and discussion

In this section, the most relevant results obtained during the commissioning, start-up, and full integration of the prototype described in the "Pilot plant layout and main features" sub-section are presented. The operation of the system has been divided into three main parts: (1) validation of SGE-RED pilot plant under site-specific conditions, (2) analysis of the influence of operating conditions with synthetic solutions, and (3) operation with real streams of seawater and treated WW.

3.1. Commissioning and validation of the performance of the pilot plant under site-conditions

This section provides a comprehensive analysis of the performance of the up-scaled RED system using NaCl synthetic solutions with concentrations of 0.55 M for the HC compartment and 0.02 M for the LC compartment, thereby maintaining a constant salinity gradient. The results are presented for a flow rate condition of 500 L/h, keeping $Q_{LC} = Q_{HC}$ and constant temperature of 293K.

While the flow rate is an adjustable operational variable that directly impacts the ion transport and energy conversion efficiency, the temperature is governed by climate conditions, affecting the resistance to ion trans-membrane transport and decreasing the global performance. Understanding the interplay between these variables in a real scenario is crucial for enhancing the viability of RED systems in large-scale energy recovery applications.

The electrical performance of the RED units at pilot-scale was forecasted using an advanced mathematical model as described in a previous study by Ortiz-Martínez et al. (2020). This model was accurately adapted to align with the specific features of commercial RED modules from FuMATech GmbH®, ensuring realistic and reliable predictions.

Fig. 3 illustrates the correlation between power density and current intensity for a gradient of 0.55 M/0.02 M NaCl for HC and LC, respectively, combining experimental data (symbols) and simulation results (solid lines). At a flow rate of 500 L/h and a constant temperature of 293 K, the power density shows a parabolic trend, peaking at $1.18 \pm 2 \cdot 10^{-2}$ W/m², exceeding the maximum reported by Mehdizadeh et al. (2021), 0.97 W/m², obtained in a RED pilot plant using artificial seawater (0.57M NaCl) and river water (0.004M NaCl).

The consistency between experimental and simulated results further

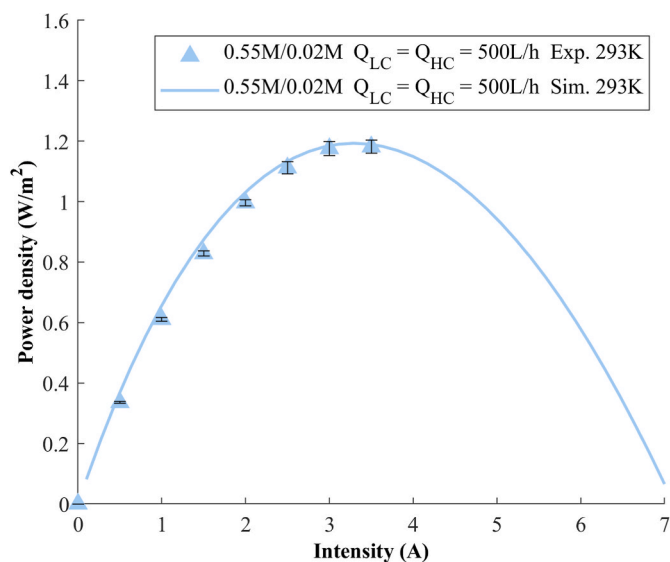


Fig. 3. Comparison of experimental and simulated power density (W/m²) as a function of current intensity (A) for a flow rate of 500 L/h and temperature of 293K. Symbols represent experimental data (Exp.), and lines indicate simulated results (Sim.).

validates the reliability of the simulations for predicting the system performance under diverse operational scenarios. Together, these results highlight the accuracy of our modelling approach in capturing the behaviour of the up-scaled technology in a real-world scenario. The data align with model predictions, thereby demonstrating the viability of the LIFE 3E proposal and validating the operation of the pilot plant.

3.2. Influence of operating conditions on the performance of the pilot plant

Once the viability of the pilot plant has been demonstrated under a range of operating conditions that are feasible within the selected site, the study examines key variables, including flow rates and temperatures, across specific ranges to understand their impact on the performance of the system. The operating conditions evaluated include temperatures between 285 and 293 K and flow rates between 500 and 1500 L/h, which correspond to the maximum and minimum flowrate values acceptable for the installation based on the characteristics of the pumping equipment. The solutions used in these experiments include synthetic NaCl solutions (equivalent to 0.55 M for HC and 0.02 M for LC) and engineered synthetic solutions with divalent ions, designed to replicate the ion composition of natural seawater and reclaimed water. After determining the influence of these variables, we can optimize the adjustable operational parameters for enhanced efficiency and power generation in the pilot plant.

3.2.1. Analysis of LC/HC flow rate ratio

Fig. 4 compares the influence of LC/HC volumetric flow rate ratio on the performance in terms of power density as a function of the applied load. The experimental and simulated data are represented under two distinct conditions: (1) when the low concentration flow rate (Q_{LC}) is equal to the high concentration flow rate (Q_{HC}), and (2) when Q_{LC} is twice Q_{HC} ($Q_{LC} = 2 \cdot Q_{HC}$). The error bars indicate the standard deviation from the experimental measurements, emphasizing the reliability and precision of the data.

The power density reaches its peak at different intensities for each condition. For the condition $Q_{LC} = Q_{HC}$, the peak power density is lower compared to the condition where $Q_{LC} = 2 \cdot Q_{HC}$. This suggests that increasing the low concentration flow rate relative to the high concentration flow rate can enhance the power density output. It is worth noting that, by doubling the LC flow rate relative to the HC pumping

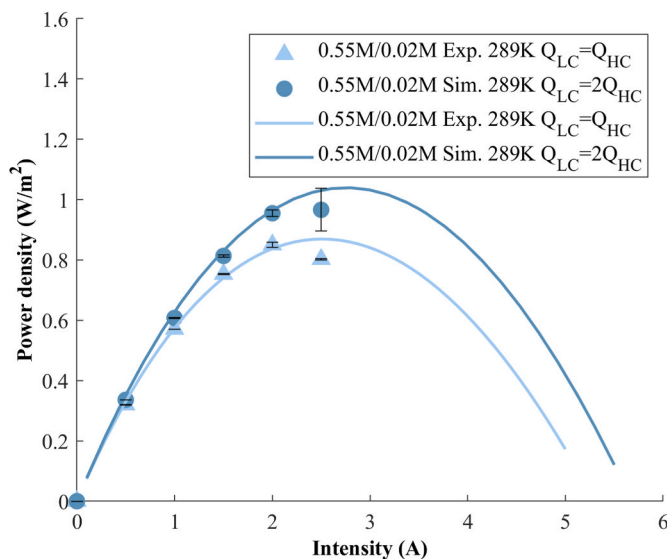


Fig. 4. Gross power density as a function of intensity for experimental and simulated data at a temperature of 289K under different flow rates ratios: $Q_{LC} = Q_{HC} = 500$ L/h and $Q_{LC} = 2Q_{HC} = 1000$ L/h.

represents up to a 20% increase in the maximum power extracted per membrane cell pair area. The simulation curves closely follow the experimental trend, validating the accuracy of the mathematical model. These results point to a trade-off between the energy performance of the RED unit and the pumping requirements associated with the flow dynamics.

3.2.2. Effect of temperature

Fig. 5 presents the analysis of the influence of temperature on the open circuit voltage (OCV) and the corresponding gross power density (W/m^2) in the RED pilot-plant installed in the UWWTP of Comillas. Attending to OCV (Fig. 5a) experimental results, at lower temperatures (285 K) it ranges from 14.46 V at a flow rate of 500 L/h to 14.94 V at 1000 L/h. As temperature rises to 293 K, the OCV values exhibit a slight increase up to 16.67 V at 1000 L/h. This trend indicates a moderate enhancement of the osmotic gradient across the membrane pairs with increasing flow rate and temperature, thereby improving the ability of the system to generate voltage. Moreover, this behaviour denotes that increased flow rates enhance ion transport and temperature raise improves ionic mobility and reduces electrical membrane resistance, thereby improving energy extraction. The dynamic response of the system corresponds to the laboratory-scale behaviour of RED technology, as reported in the literature (Mei and Tang, 2018; Tufa et al., 2018).

In Fig. 5b, the impact of temperature and flow rate on gross power density is further exposed. At the lowest temperature (285 K) and flow rate (500 L/h), the power density is observed to be $0.76 \pm 2 \cdot 10^{-2} \text{ W}/\text{m}^2$, which slightly increases to $0.81 \pm 7 \cdot 10^{-2} \text{ W}/\text{m}^2$ for a flow rate of 1000 L/h. Nonetheless, as temperature rises to 293 K, gross power density significantly increases, reaching $1.18 \pm 2 \cdot 10^{-2} \text{ W}/\text{m}^2$ at 500 L/h and peaking at $1.39 \pm 4 \cdot 10^{-3} \text{ W}/\text{m}^2$ at 1000 L/h. These results underscore that temperature has a more pronounced effect on the power output of the system compared to flow rate, with optimal performance observed at higher temperatures and increased flow rates. Therefore, these effects align with the main conclusions obtained in previous studies using synthetic NaCl solutions, which evidenced that there were no significant changes in OCV with temperature and reported a sharp increase in P_d as a function of temperature (Abdullah Shah et al., 2023).

The comparative analysis between the representations of Fig. 5 indicates a direct correlation between increased flow rates and temperatures with enhanced OCV and power density, demonstrating the sensitivity of the performance to these operational parameters. The electrochemical potential difference between the RED stack electrodes is positively influenced by the volumetric flow rate and temperature, with the latter having a more significant impact. However, temperature notably limits the maximum power density achieved under load,

primarily due to its effect on the internal resistance and selectivity of the membranes. Previously, Guo et al., 2018 examined the effects of temperature on RED obtaining a similar upward trend in both OCV and P_d when increasing temperature from 25 °C to 60 °C, attributed to the increased electrochemical potential and the reduced internal resistance of the stack components. This is consistent with the observations in the RED pilot-plant at Comillas, which also demonstrated the improvement in the performance metrics with increasing temperature.

3.2.3. Effect of divalent ions

The next phase of the demonstration activities at the LIFE 3E pilot plant has focused on experiments with synthetic seawater and treated WW designed based on the ionic characterization provided in Table 2. Fig. 6 illustrates the effect of the presence of multivalent ions and temperature on power density of RED systems.

Divalent ions such as Ca^{2+} , Mg^{2+} , and SO_4^{2-} present in real-world water sources detrimentally affect the generation of salinity gradient energy. These ions increase membrane resistance, thereby reducing the ionic flux (Gómez-Coma et al., 2019). The negative impact of multivalent ions, which can result in a reduction of power density (P_d) by approximately 10–15%, is most pronounced under more favourable temperature conditions (290–293K), with P_d decreasing from $1.07 \pm 4 \cdot 10^{-3} \text{ W}/\text{m}^2$ to $0.96 \pm 5 \cdot 10^{-3} \text{ W}/\text{m}^2$ (Fig. 6a).

Fig. 6b shows the decrease in power obtained in the presence of real-world streams salt compositions. However, in the lower temperature range of 286–289K, the declining impact of multivalent salts is practically mitigated, with the peak power density only slightly decreasing from $0.85 \pm 8 \cdot 10^{-3} \text{ W}/\text{m}^2$ to $0.82 \pm 3 \cdot 10^{-2} \text{ W}/\text{m}^2$.

The experimental data across both figures indicate that the presence of divalent ions consistently reduces RED performance regardless of temperature, highlighting the need for ion-selective membranes (Sun et al., 2024) and optimized operational strategies to mitigate these adverse effects. This is consistent with the main conclusions reported in literature so far, which indicate that increased temperature generally enhances ion mobility and reduces resistance, thereby improving power output (Veerman et al., 2023).

The validated simulation model provides a solid foundation to serve as a powerful tool for further optimization and scale-up studies of RED systems. It can reliably predict RED system performance, accounting for various operational parameters such as temperature and ionic composition. These results provide valuable insights for optimizing RED systems in practical applications, particularly in coastal wastewater treatment plants where both seawater and treated WW are readily available.

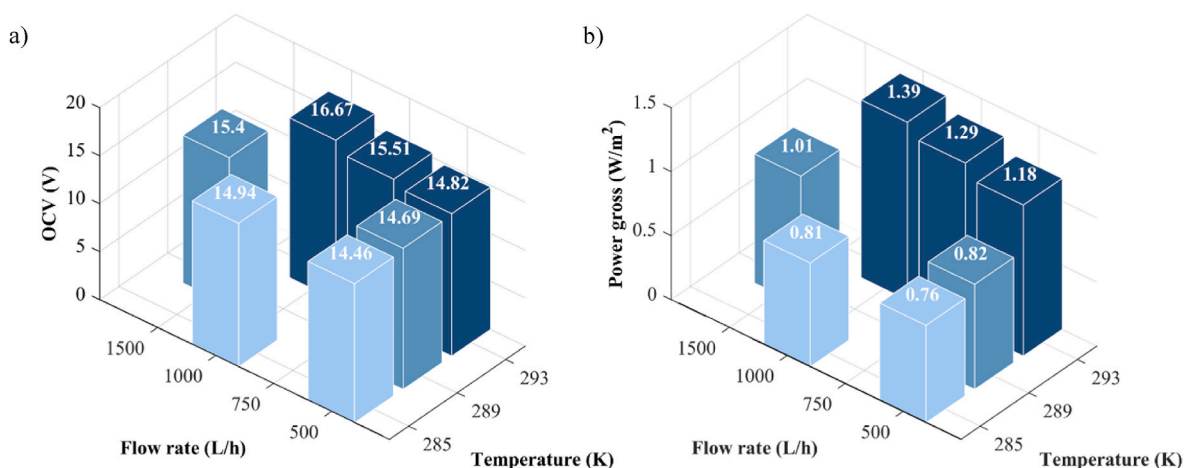


Fig. 5. Effect of flow rate (L/h) and temperature (K) on open circuit voltage (a) (OCV, V) and gross power density (b) (W/m^2).

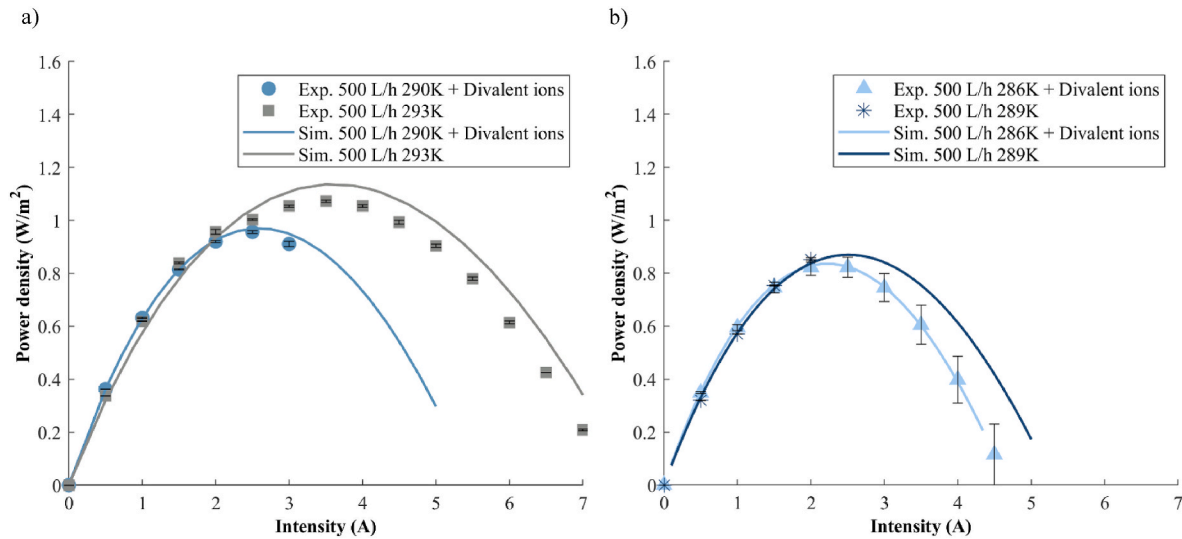


Fig. 6. Power density (W/m²) curves as a function of intensity (A) for experimental and simulated data at different ranges of temperature (a) (293–290K) and (b) (286–289K) comparing synthetic NaCl streams and synthetic multivalent ions solutions. Operating conditions: $Q_{LC} = Q_{HC} = 500$ L/h.

3.2.4. Accuracy of the SGE-RED model under pilot plant conditions

The parity plot of Fig. 7 illustrates the validation of the mathematical model, previously supported at the laboratory scale by Ortiz-Martínez et al. (2020), now tested under pilot plant conditions for reverse electro dialysis (RED). The x-axis shows the experimentally measured power density, while the y-axis displays the simulated power density (in W/m²). Each data point represents a distinct experimental operating condition.

The solid diagonal line represents the ideal scenario where the simulated values perfectly match the experimental values. The dashed lines indicate a $\pm 15\%$ deviation from the ideal line, providing a visual representation of the accuracy of the model and robustness under real-world conditions. Most data points fall within this acceptable error range, demonstrating the high level of agreement between simulated and experimental results. This agreement supports the validity of the model and reliability in predicting the performance of RED systems at the pilot plant scale.

The parity plot of experimental versus simulated gross power density (P_d) values, with a range of experimental values from 0.76 to 1.39 W/

m², demonstrates the high accuracy and reliability of the adapted mathematical model for pilot-scale SGE-RED systems. The Root Mean Square Error (RMSE) value of 0.075 W/m² indicates that the predicted values with the model deviate minimally from the observed data, representing approximately 11.9% of the data range. This statistical indicator has been calculated using the expression defined in Eq. (1) for n number of data points ($n = 23$). This small deviation underscores the robustness of the model, as it accurately reflects the experimental outcomes with a low margin of error. Recent studies have emphasized the importance of accurate modelling for optimizing RED system performance and scaling up from laboratory to industrial applications (Sampedro et al., 2023). The model, initially validated at the laboratory scale, has been effectively readapted for pilot-scale operations, confirming its capability to reliably predict power density under varying operational conditions such as HC and LC flow rate, temperature and salts molarity. This high level of precision is crucial for optimizing reverse electro dialysis systems, as it ensures that the simulated values can be trusted to make informed decisions for real-world applications and LIFE 3E technology replicability in other water treatment facilities.

$$RMSE = \sqrt{\frac{1}{n} \sum_{i=1}^n (P_{d,Exp} - P_{d,Sim})^2} \quad \text{Eq. (1)}$$

3.3. Prototype testing with real waters

The final experimental phase of this work for the LIFE 3E concept demonstration in a real WWTP at a pilot plant scale involved testing real-world water streams. Table 3 presents the physico-chemical characteristics of seawater and treated WW streams used in the operation.

These characteristics are crucial for understanding the performance and efficiency of the reverse electro dialysis system under real-world environmental conditions. The low BOD₅ values for both water inputs indicate minimal organic pollution, which is favourable for maintaining membrane performance and preventing fouling (Mejía-Marchena et al., 2023; Vermaas et al., 2013). The higher turbidity in the treated wastewater implies a higher load of particulate matter, which could potentially lead to more frequent cleaning cycles or pre-treatment steps to ensure efficient operation of the RED system.

3.3.1. Results

Fig. 8 reports the comparison of experimental datasets for the testing conducted with (1) synthetic solutions with divalent ions (●) and (2) natural waters (✱), along with their corresponding simulated P_d vs. I

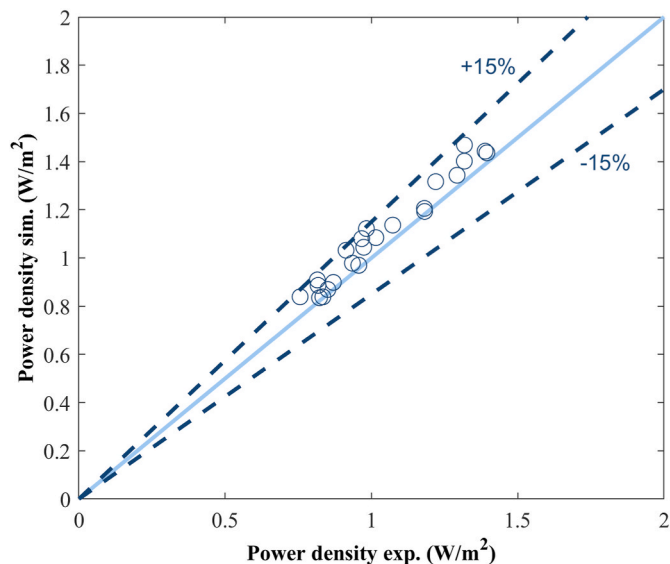


Fig. 7. Parity plot comparing simulated and experimental maximum power densities for the pilot-scale RED system.

Table 3
Characteristics of seawater and treated WW streams.

	Cond. (mS/cm)	pH (-)	BOD ₅ (mg/L O ₂)	TOC (mg/L)	Turbidity (NTU)	TSS (mg/L)	TDS (mg/L)
Seawater	47.95 ± 3.4	7.84 ± 0.15	<10	<10 (2.7)	0.96	6 ± 1.4	33,275
Treated WW	0.785 ± 0.1	7.06 ± 0.15	<10	9.9	3.2	<5.0	466

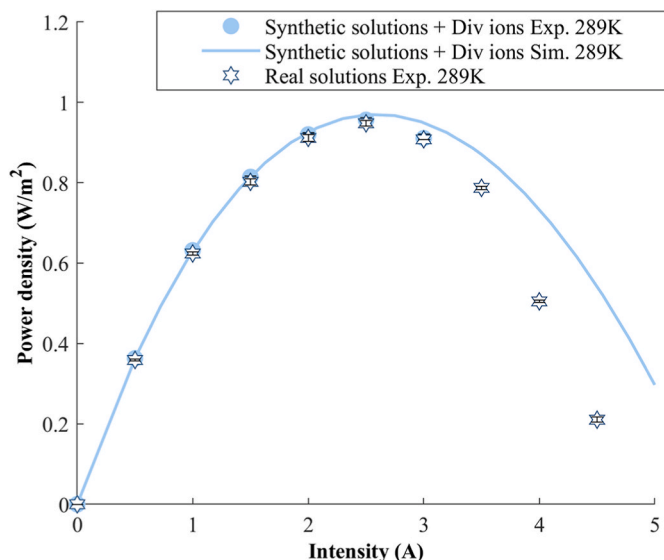


Fig. 8. RED system power curves for different feed solutions. Operating conditions: $Q_{LC} = Q_{HC} = 500$ L/h and a salinity gradient for synthetic solutions with divalent ions equivalent to seawater and treated WW streams and natural solutions.

curve. Real-world streams, which are more representative of actual operational conditions, show slightly lower performance compared to synthetic solutions, decreasing from $0.96 \pm 5 \cdot 10^{-3}$ W/m², to $0.95 \pm 7 \cdot 10^{-3}$ W/m² at an intensity near 2.5 A. This performance drop can be

attributed to the presence of multivalent ions, organic matter, and other impurities, which can affect ion exchange efficiency and membrane fouling. These results emphasize the need for robust pre-treatment processes equivalent to wastewater tertiary treatments to remove or mitigate the impact of such contaminants.

3.3.2. SGE-RED performance indicators

In this section, we present the results of our experimental investigations focusing on the performance indicators SGE-RED. The subsequent parts detail the definitions and analyses of the performance meters used in this study, providing a comprehensive comparison of the RED pilot efficiency with previous studies.

3.3.2.1. Meters definition. Generally, the performance of reverse electrodialysis for energy extraction is reflected through the maximum power density achieved, i.e., power (W) per membrane pair area (m²). However, in the water treatment industry, energy requirements are typically expressed in terms of electrical energy per cubic meter of processed water. To address both needs, in this work, maximum performances have been expressed and compared as: (1) power per membrane cell pair area (W/m²), (2) energy generated per volume of regenerated water (Wh/m³_{LC}), and (3) energy generated per volume of regenerated water and membrane cell pair area (Wh/m²·m³_{LC}).

3.3.2.2. Analysis of the monitored results. The performance of reverse electrodialysis (RED) for energy extraction was evaluated by comparing the power density and energy generation across different flow rates using pure NaCl solutions, synthetic solutions with divalent ions, and natural solutions. Fig. 9 depicts the results of the energy performance indicators defined in this work and compares them with other pilot-scale

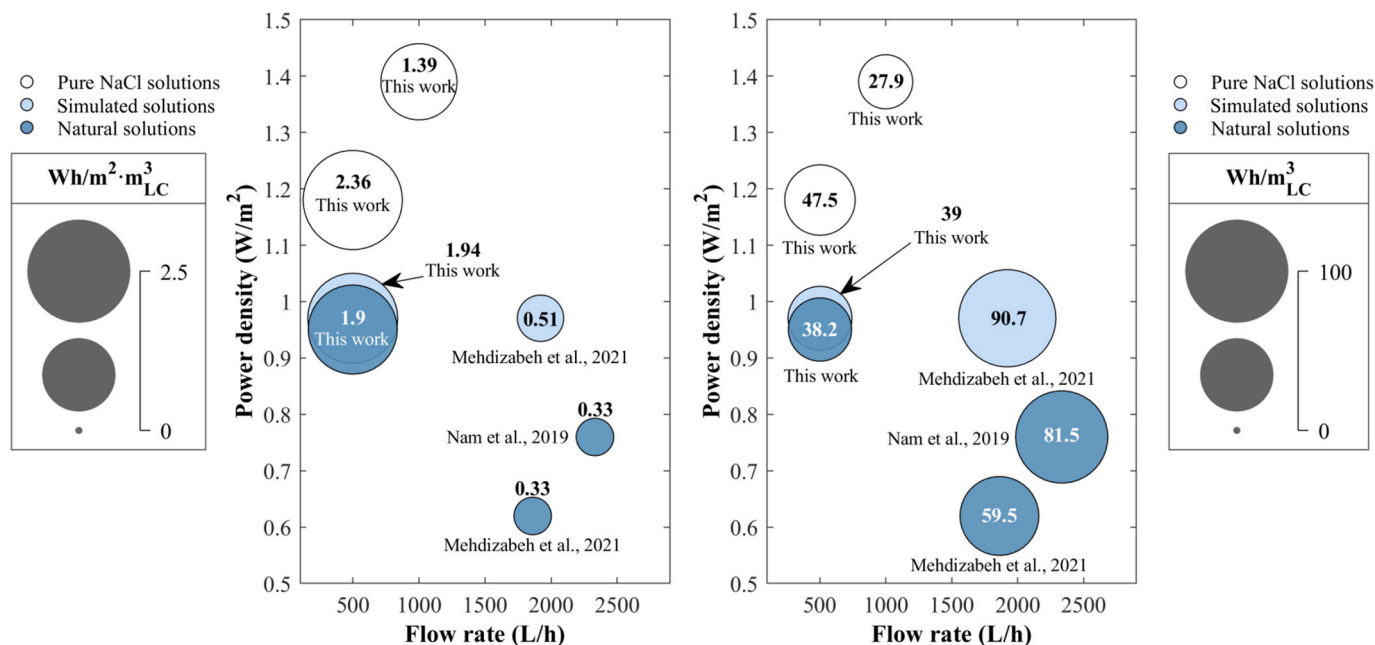


Fig. 9. Comparison of performance indicators for energy harvesting from the gradient between seawater and treated wastewater as function of power density (W/m²) and across different flow rates (L/h) using pure NaCl solutions, simulated solutions, and natural solutions. a) The bubbles show the energy extracted per cell pair membrane area and LC volume (Wh/m²·m³_{LC}). b) The bubbles illustrate the energy generated per LC volume treated (Wh/m³_{LC}). The size of the bubbles represents the magnitude of the performance indicator.

studies that also aim to extract SGE-RED from seawater and treated wastewater. This representation evidences the correlation between flow rate and power output in different pilot systems.

The results indicate that our study, represented by the data points labelled "This work" demonstrates competitive power densities and energy generation metrics. Specifically, for pure NaCl solutions, our system achieved a maximum power efficiency of $2.36 \text{ W/m}^2 \cdot \text{m}^3_{\text{LC}}$ at a flow rate of $Q_{\text{LC}} = Q_{\text{HC}} = 500 \text{ L/h}$ with a power density of $1.18 \pm 2 \cdot 10^{-2} \text{ W/m}^2$. In terms of energy generated per volume of LC water, our system achieved up to $47.5 \text{ Wh/m}^3_{\text{LC}}$.

For synthetic solutions and $Q_{\text{LC}} = Q_{\text{HC}} = 500 \text{ L/h}$, our work achieved a power density of $0.96 \pm 5 \cdot 10^{-3} \text{ W/m}^2$, which translates into $1.94 \text{ W/m}^2 \cdot \text{m}^3_{\text{LC}}$ and $39 \text{ Wh/m}^3_{\text{LC}}$, showcasing the potential of our RED system with simulated water compositions. These data are comparable to the study by [Mehdizadeh et al. \(2021\)](#) which reports higher energy extraction per volume of water synthetic solutions fed to the RED stack, achieving $90.7 \text{ Wh/m}^3_{\text{LC}}$. Nonetheless, their performance based on the available ion exchange membrane area reduces the second indicator to $0.51 \text{ Wh/m}^2 \cdot \text{m}^3_{\text{LC}}$.

Regarding the operation of RED pilot-scale systems with real-world solutions, the present study reports a power density of $0.95 \pm 7 \cdot 10^{-3} \text{ W/m}^2$. This reflects an energy efficiency per membrane area and reclaimed water flow rate of $1.9 \text{ W/m}^2 \cdot \text{m}^3_{\text{LC}}$ generating up to $38.2 \text{ Wh/m}^3_{\text{LC}}$. These results demonstrate the effectiveness of the designed prototype with a commercial RED module of 20.125 m^2 cell pair membrane area.

When comparing these results with those of [Mehdizadeh et al. \(2021\)](#) and [Nam et al. \(2019\)](#), several key points emerge. Mehdizadeh et al. reported power density of 0.62 W/m^2 , energy efficiency per membrane area and reclaimed water flow rate of $0.33 \text{ W/m}^2 \cdot \text{m}^3_{\text{LC}}$, and energy generation of $59.5 \text{ Wh/m}^3_{\text{LC}}$ with 179.4 m^2 membrane area. This result indicates potential inefficiencies in membrane utilization or higher resistances within their system.

Nam et al. reported power density of 0.76 W/m^2 , energy efficiency of $0.33 \text{ W/m}^2 \cdot \text{m}^3_{\text{LC}}$, and energy generation of $81.5 \text{ Wh/m}^3_{\text{LC}}$ with 250 m^2 membrane area. Noticeably, these research publications reported lower power densities and energy generation values, emphasizing the superior performance of our RED system across different water characteristics and flow rates. These results validate the efficiency and scalability of our approach for sustainable energy extraction from salinity gradients.

Our study demonstrates a significantly higher power density and energy efficiency per membrane area compared to Mehdizadeh et al. and Nam et al., despite utilizing a considerably smaller membrane area. This discrepancy could be attributed to differences in the systems configuration, operational conditions, and the composition of the real-world solutions. This highlights the strength of the design of the pilot prototype and operational parameters in achieving superior power densities to those previously reported.

The comparative analysis highlights the trade-offs between power density, efficiency per membrane area, and energy generation per volume of water and membrane area in RED systems. This work presents a balanced performance with higher power density and efficiency, offering a robust design suitable for real-world environmental applications. Future work should focus on optimizing operational conditions and system configurations to enhance both performance indicators, thereby improving the overall efficiency of RED systems.

4. Conclusions

A successful commissioning and start-up of a SGE-RED pilot plant located in Comillas UWWTP (Cantabria, Spain) to satisfy the energy requirements for the production of $1.0 \text{ m}^3/\text{h}$ of reclaimed water has been presented in detail. In a first step, the pilot plant performance has been validated under different operation conditions using a high accuracy and reliability advanced mathematical model.

Even in the presence of multivalent ions and other impurities, which

typically increase membrane resistance and reduce ionic flux, the RED system maintained competitive power density. Specifically, the power density achieved with seawater and treated urban wastewater as high and low concentrated streams was $0.95 \pm 7 \cdot 10^{-3} \text{ W/m}^2$, only slightly lower than the value obtained operating with synthetic solutions.

Comparative analysis with other pilot-scale studies highlights the superior efficiency of the RED equipment in this work, despite utilizing a smaller membrane area. Specifically, our system achieved a power efficiency of $2.36 \text{ W/m}^2 \cdot \text{m}^3_{\text{LC}}$ and $47.5 \text{ Wh/m}^3_{\text{LC}}$ with pure NaCl solutions, and $1.9 \text{ W/m}^2 \cdot \text{m}^3_{\text{LC}}$ and $38.2 \text{ Wh/m}^3_{\text{LC}}$ with real-world water streams. Thus, to the best of our knowledge this RED pilot plant, integrated within a real wastewater treatment plant (WWTP), is pioneering in its nature.

These results underscore the effectiveness of the prototype in generating sustainable energy from salinity gradients and demonstrate its scalability for real-world applications. However, long-term experiments are necessary to validate these findings thoroughly, ensuring the reliability and efficiency of the RED system over extended periods.

Nomenclature

b	Channel width
cp	Cell pair
L	Channel length
N_{cp}	Number of cell pairs
P_d	Power density (W/m^2)
R_0	Electrical resistance
α_{AEM}	Permselectivity
α_{CEM}	Permselectivity
δ	Thickness dry
δ_{sp}	Inter-membrane distance equal to spacer's thickness
ϵ	Spacer's porosity
Q	Volumetric flow rate (m^3/h)
T	Temperature (K)
Abbreviation	
RED	Reverse electrodialysis
WWTP	Wastewater treatment plant
SGE	Salinity Gradient Energy
AEM	Anion Exchange Membrane
CEM	Cation Exchange Membrane
TOC	Total Organic Carbon
HC	High-concentrated
ERS	Electrode rinse solution
TSS	Total Suspended Solids
TDS	Total Dissolved Solids
BOD_5	Biological Oxygen Demand
LC	Low-concentrated
WW	Wastewater

CRedit authorship contribution statement

Tamara Sampedro: Writing – original draft, Visualization, Investigation, Formal analysis. **Elisa Mazo:** Validation, Methodology, Investigation. **Lucía Gómez-Coma:** Writing – review & editing, Software, Conceptualization. **Axel Arruti:** Resources, Conceptualization. **Marcos Fallanza:** Software, Methodology, Conceptualization. **Javier Pinedo:** Resources, Conceptualization. **Javier Rioyo:** Project administration, Conceptualization. **María Sainz:** Funding acquisition, Conceptualization. **Raquel Ibañez:** Writing – review & editing, Supervision, Project administration. **Inmaculada Ortiz:** Writing – review & editing, Supervision, Funding acquisition.

Declaration of competing interest

The authors declare that they have no known competing financial interests or personal relationships that could have appeared to influence the work reported in this paper.

Acknowledgements

This research work is supported by the European LIFE Programme (LIFE19 ENV/ES/000143), the project PDC2021-120786-I00 financed by MICIU/AEI/10.13039/501100011033 and European Union Next Generation EU/RTRP, and the project PID2020-115409RB-I00 financed by MICIU/AEI/10.13039/501100011033.

Data availability

Data will be made available on request.

References

- Abdullah Shah, S., Cucchiara, R., Vicari, F., Cipollina, A., Tamburini, A., Micale, G., 2023. Energetic valorisation of saltworks bitterns via reverse electro dialysis: a laboratory experimental campaign. *Membranes* 13. <https://doi.org/10.3390/membranes13030293>.
- Cardoso, B.J., Rodrigues, E., Gaspar, A.R., Gomes, Á., 2021. Energy performance factors in wastewater treatment plants: a review. *J. Clean. Prod.* <https://doi.org/10.1016/j.jclepro.2021.129107>.
- Chae, S., Kim, H., Gi Hong, J., Jang, J., Higa, M., Pishnamazi, M., Choi, J.Y., Chandula Walgama, R., Bae, C., Kim, I.S., Park, J.S., 2023. Clean power generation from salinity gradient using reverse electro dialysis technologies: recent advances, bottlenecks, and future direction. *Chem. Eng. J.* <https://doi.org/10.1016/j.cej.2022.139482>.
- Choi, P.J., Lee, J., Jang, A., 2024. Interconnection between renewable energy technologies and water treatment processes. *Water Res.* <https://doi.org/10.1016/j.watres.2024.122037>.
- Gómez-Coma, L., Ortiz-Martínez, V.M., Carmona, J., Palacio, L., Prádanos, P., Fallanza, M., Ortiz, A., Ibañez, R., Ortiz, I., 2019. Modeling the influence of divalent ions on membrane resistance and electric power in reverse electro dialysis. *J. Membr. Sci.* 592. <https://doi.org/10.1016/j.memsci.2019.117385>.
- Gómez-Coma, L., Ortiz-Martínez, V.M., Fallanza, M., Ortiz, A., Ibañez, R., Ortiz, I., 2020. Blue energy for sustainable water reclamation in WWTPs. *J. Water Process Eng.* 33. <https://doi.org/10.1016/j.jwpe.2019.101020>.
- Guo, Z.Y., Ji, Z.Y., Zhang, Y.G., Yang, F.J., Liu, J., Zhao, Y.Y., Yuan, J.S., 2018. Effect of ions (K⁺, Mg²⁺, Ca²⁺ and SO₄²⁻) and temperature on energy generation performance of reverse electro dialysis stack. *Electrochim. Acta* 290, 282–290. <https://doi.org/10.1016/j.electacta.2018.09.015>.
- Gurreri, L., Tamburini, A., Cipollina, A., Micale, G., 2020. Electro dialysis applications in wastewater treatment for environmental protection and resources recovery: a systematic review on progress and perspectives. *Membranes* 10, 1–93. <https://doi.org/10.3390/membranes10070146>.
- Hong, J.G., Park, T.W., 2023. Ion-exchange membranes for blue energy generation: a short overview focused on nanocomposite. *J. Electrochem. Sci. Eng.* <https://doi.org/10.5599/jese.1447>.
- International Energy Agency (IEA), 2018. The energy sector should care about wastewater [WWW Document]. URL: <https://www.iea.org/commentaries/the-energy-sector-should-care-about-wastewater>, 4.29.24.
- Jones, E.R., Bierkens, M.F.P., Wanders, N., Sutanudjaja, E.H., van Beek, L.P.H., van Vliet, M.T.H., 2022. Current wastewater treatment targets are insufficient to protect surface water quality. *Commun Earth Environ* 3. <https://doi.org/10.1038/s43247-022-00554-y>.
- Jones, E.R., Van Vliet, M.T.H., Qadir, M., Bierkens, M.F.P., 2021. Country-level and gridded estimates of wastewater production, collection, treatment and reuse. *Earth Syst. Sci. Data* 13, 237–254. <https://doi.org/10.5194/essd-13-237-2021>.
- Kakwani, N.S., Kalbar, P.P., 2024. Prioritization of strategies for urban water circular economy using water circularity indicator. *Water Pol.* <https://doi.org/10.2166/wp.2024.233>.
- Li, Z., Wang, C., Liu, Y., Wang, J., 2024. Enhancing the explanation of household water consumption through the water-energy nexus concept. *NPJ Clean Water* 7. <https://doi.org/10.1038/s41545-024-00298-6>.
- LIFE 3E, 2024. Towards reclamation of coastal UWWTP effluents with energy recovery. <https://life3e.eu/home>, 6.28.24.
- Logan, B.E., Elimelech, M., 2012. Membrane-based processes for sustainable power generation using water. *Nature*. <https://doi.org/10.1038/nature11477>.
- Mehdizadeh, S., Kakihana, Y., Abo, T., Yuan, Q., Higa, M., 2021. Power generation performance of a pilot-scale reverse electro dialysis using monovalent selective ion-exchange membranes. *Membranes* 11, 1–25. <https://doi.org/10.3390/membranes11010027>.
- Mei, Y., Tang, C.Y., 2018. Recent developments and future perspectives of reverse electro dialysis technology: a review. *Desalination*. <https://doi.org/10.1016/j.desal.2017.10.021>.
- Mejía-Marchena, R., Maturana-Córdoba, A., Fernández-Rojano, S., 2023. Unveiling the enhancing potential of water pretreatment on energy efficiency in reverse electro dialysis systems - a comprehensive review. *J. Water Process Eng.* <https://doi.org/10.1016/j.jwpe.2023.104548>.
- Moreno, J., de Hart, N., Saakes, M., Nijmeijer, K., 2017. CO₂ saturated water as two-phase flow for fouling control in reverse electro dialysis. *Water Res.* 125, 23–31. <https://doi.org/10.1016/j.watres.2017.08.015>.
- Nam, J.Y., Hwang, K.S., Kim, H.C., Jeong, H., Kim, H., Jwa, E., Yang, S.C., Choi, J., Kim, C.S., Han, J.H., Jeong, N., 2019. Assessing the behavior of the feed-water constituents of a pilot-scale 1000-cell-pair reverse electro dialysis with seawater and municipal wastewater effluent. *Water Res.* 148, 261–271. <https://doi.org/10.1016/j.watres.2018.10.054>.
- Ortiz-Martínez, V.M., Gómez-Coma, L., Tristán, C., Pérez, G., Fallanza, M., Ortiz, A., Ibañez, R., Ortiz, I., 2020. A comprehensive study on the effects of operation variables on reverse electro dialysis performance. *Desalination* 482. <https://doi.org/10.1016/j.desal.2020.114389>.
- Pattle, R.E., 1954. *Production of Electric Power by Mixing Fresh and Salt Water in the Hydro-Electric Pile*, vol. 174, p. 660.
- Rastgar, M., Moradi, K., Burroughs, C., Hemmati, A., Hoek, E., Sadrzadeh, M., 2023. Harvesting blue energy based on salinity and temperature gradient: challenges, solutions, and opportunities. *Chem Rev.* <https://doi.org/10.1021/acs.chemrev.3c00168>.
- Sampedro, T., Tristán, C., Gómez-Coma, L., Fallanza, M., Ortiz, I., Ibañez, R., 2023. Design of a reverse electro dialysis plant for salinity gradient energy extraction in a coastal wastewater treatment plant. *Membranes* 13. <https://doi.org/10.3390/membranes13060546>.
- Sun, X., Di, M., Gao, L., Jiang, X., Ruan, X., Yan, X., He, G., 2024. Scalable fabrication of integrated covalent organic framework membrane with selective ion transport for efficient salinity gradient energy harvesting. *Nano Energy* 128. <https://doi.org/10.1016/j.nanoen.2024.109959>.
- Tedesco, M., Cipollina, A., Tamburini, A., Micale, G., 2017. Towards 1 kW power production in a reverse electro dialysis pilot plant with saline waters and concentrated brines. *J. Membr. Sci.* 522, 226–236. <https://doi.org/10.1016/j.memsci.2016.09.015>.
- Tedesco, M., Scalici, C., Vaccari, D., Cipollina, A., Tamburini, A., Micale, G., 2016. Performance of the first reverse electro dialysis pilot plant for power production from saline waters and concentrated brines. *J. Membr. Sci.* 500, 33–45.
- Tow, E.W., Hartman, A.L., Jaworowski, A., Zucker, I., Kum, S., AzadiAghdam, M., Blatchley, E.R., Achilli, A., Gu, H., Urper, G.M., Warsinger, D.M., 2021. Modeling the energy consumption of potable water reuse schemes. *Water Res. X.* <https://doi.org/10.1016/j.wroa.2021.100126>.
- Tristán, C., Fallanza, M., Ibañez, R., Ortiz, I., Grossmann, I.E., 2023. A generalized disjunctive programming model for the optimal design of reverse electro dialysis process for salinity gradient-based power generation. *Comput. Chem. Eng.* 108196. <https://doi.org/10.1016/j.compchemeng.2023.108196>.
- Tufa, R.A., Pawlowski, S., Veerman, J., Bouzek, K., Fontananova, E., di Profio, G., Velizarov, S., Goulão Crespo, J., Nijmeijer, K., Curcio, E., 2018. Progress and prospects in reverse electro dialysis for salinity gradient energy conversion and storage. *Appl. Energy*. <https://doi.org/10.1016/j.apenergy.2018.04.111>.
- UN environment programme, 2023. *Water-energy Nexus in Urban Water Supply Systems ISSUE BRIEF*.
- United Nations, 2024. *The United Nations World Water Development Report 2024: Water for Prosperity and Peace*. UNESCO, Paris. UNITED NATIONS EDUCATIONA.
- United Nations, 2023. *The Sustainable Development Goals Report 2023*.
- United Nations, 2021. *UNITED NATIONS WORLD WATER DEVELOPMENT REPORT 2021: Valuing Water*. UNESCO, Paris. UNITED NATIONS EDUCATIONA.
- United Nations Environment Programme, 2023. *Wastewater - turning problem to solution*. A UNEP rapid response assessment. <https://doi.org/10.59117/20.500.11822/43142>.
- Veerman, J., Gómez-Coma, L., Ortiz, A., Ortiz, I., 2023. Resistance of ion exchange membranes in aqueous mixtures of monovalent and divalent ions and the effect on reverse electro dialysis. *Membranes* 13, 322. <https://doi.org/10.3390/membranes13030322>.
- Vermaas, D.A., Kunteng, D., Saakes, M., Nijmeijer, K., 2013. Fouling in reverse electro dialysis under natural conditions. *Water Res.* 47, 1289–1298. <https://doi.org/10.1016/j.watres.2012.11.053>.
- Vital, B., Baron, A.M., Kuntke, P., Gagliano, M.C., Hamelers, H.V.M., Sleutels, T., 2024. Evaluation of chemical free cleaning techniques for reverse electro dialysis stacks fed with natural waters. *J. Water Process Eng.* 61. <https://doi.org/10.1016/j.jwpe.2024.105236>.
- WWAP (United Nations World Water Assessment Programme), 2017. *The United Nations World Water Development Report 2017. Wastewater: the Untapped Resource*. UNESCO, Paris.